2019 American Control Conference (ACC)
Philadelphia, PA, USA, July 10-12, 2019

An $\mathcal{H}_-/\mathcal{H}_\infty$ blending for mode decoupling

Tamás Baár and Tamás Luspay

***Abstract*— A novel input and output blend calculation method is presented for decoupled control of selected modes. Decoupling is carried out by maximizing the minimum sensitivity of the controlled mode while minimizing the worst case gain for other mode(s) from the blended input to the blended output. This leads to an optimization problem of joint maximization of the $\mathcal{H}_-$ index of the controlled mode and the minimization of the $\mathcal{H}_\infty$ norm corresponding to other modes. The optimization problem is formalized with Linear Matrix Inequalities, and two examples from the aerospace engineering field are given for evaluation purposes.**

I. INTRODUCTION

In the control of multivariable complex systems it is often desirable to have a control approach which assures the control of a certain fraction of the system, while does not affect it's other parts [1]. This objective immediately calls for the modal form of a Linear Time Invariant (LTI) system. In modal coordinates, the system dynamics has a decoupled structure: the system is modeled as a set of dynamically independent modes, where coupling appears only through the mutual input and output channels. Due to this coupling, the control of individual modes without affecting another one is a challenging engineering task.

In order to quantitatively analyze a given mode's input and output channels, [2] has introduced placement matrices based on the $\mathcal{H}_2$, $\mathcal{H}_\infty$ and Hankel norms of the system. The approach is suitable for input and output selection for systems consisting of lightly damped stable modes. The placement problem is formalized as finding a smaller subset of inputs and outputs for which the selected norm of the subset is as close as possible to the original set. The placement matrix depicts the importance of each sensor (or actuator) and each mode. Each column represents the sensor (or actuator) importance for every mode, while each row represents the mode importance for every sensor measurement. The method has been applied in [3], [4], and [5] among others.

In recent years various approaches were introduced in order to assure decoupled control of selected modes. The common point of many of these methods is that they introduce input and output blending vectors to decouple modes and reduce the control design into a Single Input Single Output (SISO) problem accordingly. [6] determines an optimal blend for the measurements which assures the isolation of the selected mode, and simultaneously computes an optimal blend for multiple control inputs to suppress the selected mode via a negative optimal feedback, and minimize the control's effect on other modes. [7] introduces a joint $\mathcal{H}_2$ norm based input and output blend calculation method which assures the controllability, observability and the independent control of selected modes.

The current paper presents a novel sensor and actuator blending approach for LTI systems, in order to assure decoupled control of individual modes. Our approach is based on the $\mathcal{H}_-$ index and the $\mathcal{H}_\infty$ norm of the system. The $\mathcal{H}_-$ index [8] is a sensitivity measure widely used in fault detection. It is based on the smallest nonzero singular value of a transfer function matrix over a given frequency range. By its maximization between given inputs and outputs the system's sensitivity can be increased. Oppositely, the $\mathcal{H}_\infty$ norm defines the maximal singular value of a transfer function matrix and it is mainly used in robust analysis and synthesis problems [9]. By minimizing the $\mathcal{H}_\infty$ norm, the maximum sensitivity of the transfer function matrix is minimized. The present approach seeks input and output blend vectors which are maximizing the sensitivity for a given mode, while minimizing it for another one. This way decoupling can be achieved and consequently a suitably designed control law will affect one mode, while leaving unattained the other one(s).

The outline of the paper is as follows. Section II contains the problem statement, while Section III provides the necessary mathematical tools. The main results are presented in Section IV, which are evaluated by numerical examples in Section V. The paper is concluded in Section VI.

II. PROBLEM STATEMENT

Consider a stable, diagonalizable LTI system given in the following generic state space form

$$\begin{aligned} \dot{x}(t) &= Ax(t) + Bu(t), \\ y(t) &= Cx(t) + Du(t), \end{aligned} \tag{1}$$

with the standard notations: $x(t) \in \mathbb{R}^n$ is the state vector, $u(t) \in \mathbb{R}^m$ is the input vector and $y(t) \in \mathbb{R}^p$ is the output vector of the system. We assume that the system is given in its modal form, with

$$\begin{aligned} A &= \begin{bmatrix} A_1 & 0 & \dots & 0 \\ 0 & A_2 & \dots & 0 \\ \vdots & \vdots & \vdots & \vdots \\ 0 & \dots & 0 & A_N \end{bmatrix}, \quad B = \begin{bmatrix} B_1 \\ B_2 \\ \vdots \\ B_N \end{bmatrix}, \\ C &= \begin{bmatrix} C_1 & C_2 & \dots & C_N \end{bmatrix}. \end{aligned} \tag{2}$$

Here N refers to the number of modes in the system. Dynamical modes can be represented by either real ($\Re$) or complex (with imaginary part $\Im$) eigenvalues (λ), which determines the structure of the block-matrix A as

$$A_i = \begin{cases} \lambda_i & \text{if} \quad \Im(\lambda_i) = 0 \\ \begin{bmatrix} \Re(\lambda_i) & \Im(\lambda_i) \\ -\Im(\lambda_i) & \Re(\lambda_i) \end{bmatrix} & \text{if} \quad \Im(\lambda_i) \neq 0. \end{cases} \tag{3}$$

Under the assumption of diagonalizable A, (3) is always achievable with respective similarity transformation.

The transfer function matrix representation is given by

$$\mathcal{G}(s) = \sum_{i=1}^{N} C_i (sI - A_i)^{-1} B_i + D = \sum_{i=1}^{N} M_i(s) + D, \tag{4}$$

The authors are with the Systems and Control Lab, Institute for Computer Science and Control, Hungarian Academy of Sciences, H-1111 Budapest, Hungary. baar.tamas@sztaki.mta.hu, luspay.tamas@sztaki.mta.hu

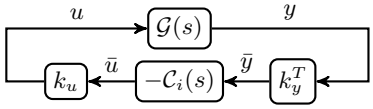

Fig. 1. Closed loop control scheme with input and output blending

where $M_i(s)$ is the transfer function of the i^{th} mode.

In the mode decoupling problem we assume that our objective is to control the i^{th} mode of the system, while leaving the j^{th} mode unattained. We intend to attain this decoupling by appropriately blending the input and output vectors of the system. For this purpose we introduce $k_u \in \mathbb{R}^{m\times 1}$ and $k_y \in \mathbb{R}^{p\times 1}$: the normalized input and output blending vectors, respectively. These blending vectors transform the $u(t)$ and $y(t)$ signal vectors onto a single dimension, therefore transforming the control problem into a SISO one. The corresponding closed loop control architecture is illustrated in Figure 1, where $\mathcal{G}(s)$ contains both the i^{th} and j^{th} modes and $\mathcal{C}_i(s)$ is a SISO controller, designed for the i^{th} mode. The input of $\mathcal{C}_i(s)$ is $\bar{y} = k_y^T y \in \mathbb{R}$ i.e. the blended scalar output of the system. The controller's output is the blended control input $\bar{u} \in \mathbb{R}$, with $u = k_u \bar{u}$.

In the paper we adopt the notions of $\mathcal{H}_\infty$ norm and the $\mathcal{H}_-$ index of the transfer function matrix $\mathcal{G}(s)$. The $\mathcal{H}_\infty$ norm is defined as

$$||\mathcal{G}(s)||_\infty := \sup_\omega \bar{\sigma}\left[\mathcal{G}(j\omega)\right], \tag{5}$$

where the frequency range is $\omega \in [0, \infty)$. It is clear that (5) is the maximum singular value of $\mathcal{G}(s)$, i.e. the maximal sensitivity from u to y. The $\mathcal{H}_-$ index is defined as

$$||G(s)||_-^{[0,\bar{\omega}]} := \inf_{\omega\in[0,\bar{\omega}]} \underline{\sigma}\left[\mathcal{G}(j\omega)\right], \tag{6}$$

with $\underline{\sigma}$ denoting the minimum singular value and $\bar{\omega}$ being the maximal frequency value of the frequency band $[0, \bar{\omega}]$. Clearly, (6) is the smallest singular value of $\mathcal{G}(s)$ and hence represents the minimal sensitivity of the system from u to y.

Now, we are in the position to formally state the blending problem as: find k_u and k_y vectors such that

$$||k_y^T G_i(s) k_u||_-^{[0,\bar{\omega}]} > \beta \tag{7}$$

is maximized, while

$$||k_y^T G_j(s) k_u||_\infty < \gamma \tag{8}$$

is minimized over a selected frequency range. β and γ are two positive constants referring the sensitivity and robustness performance levels, respectively.

III. Computation of the $\mathcal{H}_\infty$ norm and $\mathcal{H}_-$ index

This section summarizes the required mathematical tools, applied later in section IV. First the well known $\mathcal{H}_\infty$ norm presented briefly, with its Linear Matrix Inequality (LMI) formulation, followed by the $\mathcal{H}_-$ index and its computation.

A. $\mathcal{H}_\infty$ norm calculation

The $\mathcal{H}_\infty$ norm is used in the paper for characterizing the worst case gain of the transfer function matrix $\mathcal{G}_j(s)$, corresponding to the mode which should be unaffected by the controller. For various reasons, which may become clear later, we have selected an LMI based computation of the $\mathcal{H}_\infty$ norm. That is, for the system (1) the $\mathcal{H}_\infty$ norm over the $[0, \infty)$ frequency range is calculated by the Bounded Real Lemma [10], which is summarized in Lemma 1.

Lemma 1. *Let $\gamma \geq 0$ be a positive constant scalar. Then $||\mathcal{G}(s)||_\infty^{[0,\infty)} < \gamma$ if and only if there exists a positive definite symmetric $Q = Q^T \succ 0$, such that*

$$\begin{bmatrix} A^TQ + QA + C^TC & QB + C^TD \\ B^TQ + D^TC & D^TD - \gamma^2 I \end{bmatrix} \preceq 0. \tag{9}$$

The proof can be found in [10]. As a standard technique in $\mathcal{H}_\infty$ problems, frequency filters can be applied in order to emphasize specific frequency range of interest [9].

B. $\mathcal{H}_-$index calculation

The $\mathcal{H}_-$ index is a well known minimum sensitivity measure in Fault Detection Filtering, where it is mainly used for maximizing the transfer from faulty inputs to the residual signals (see i.e [11]). The following subsection summarizes its main properties and computation, based on [8]. First the $\mathcal{H}_-$ index is presented for proper systems over infinite frequency range, and then a method is given for its calculation in case of strictly proper systems, which introduces a finite frequency band. The $\mathcal{H}_-$ index is used in the paper for characterizing the minimum sensitivity of the mode to be controlled (denoted as the i^{th} mode of $\mathcal{G}(s)$ later). Again, we are using an LMI based computation.

1) Infinite frequency range:

For the system given in (1) the $\mathcal{H}_-$ index over the $[0, \infty)$ frequency range is given by Lemma 2.

Lemma 2. *Let $\beta > 0$ be a positive constant scalar. Then $||\mathcal{G}(s)||_-^{[0,\infty]} > \beta$, if and only if there exists a P such that $P = P^T$ and*

$$\begin{bmatrix} A^TP + PA + C^TC & PB + C^TD \\ B^TP + D^TC & D^TD - \beta^2 I \end{bmatrix} \succ 0. \tag{10}$$

The proof can be found in [8], and is omitted here. This formulation is suitable for proper and strictly proper systems over an infinite frequency range. However for strictly proper systems the $\mathcal{H}_-$ index is always 0. To compute the minimal sensitivity over a limited frequency range, [8] developed various frequency correction methods. Next we discuss a multiplicative correction, as our approach uses this one.

2) Finite frequency range:

Consider a strictly proper SISO system Σ, given as:

$$\begin{aligned} \dot{x}(t) &= Ax(t) + Bu(t), \\ y(t) &= Cx(t). \end{aligned} \tag{11}$$

The system can be converted into a proper system by multiplying its output by an appropriate filter of $F_M(s) = (s + \kappa)/\kappa$. Here κ denotes the zero of the filter. F_M has an infinite amplitude when $\omega \to \infty$ and an amplitude of one when $\omega = 0$. Carrying out the output multiplication gives

$$\begin{aligned} y_M(s) = \frac{1}{\kappa} s y(s) + y(s) = \frac{1}{\kappa} sCx(s) + Cx(s) = \\ = \left(\frac{1}{\kappa} CA + C\right) x(s) + \frac{1}{\kappa} CBu(s), \end{aligned} \tag{12}$$

where $y_M(s)$ is the modified system output. If $CB \neq 0$ then the augmented system is just proper, if $CB = 0$, then the procedure has to be repeated by a higher order filter. If the transfer function has a relative degree of d, then

$$F_M(s) = \frac{(s + \kappa)^d}{\kappa^d}, \tag{13}$$

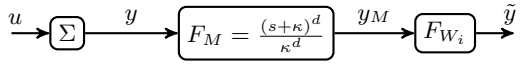

Fig. 2. Multiplicative correction of a strictly proper system to a proper one, with additional frequency weighting

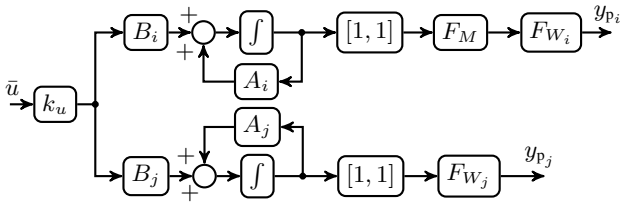

Fig. 3. Input blend calculation

converts the strictly proper system to a proper one. In case of a MIMO system, $F_M(s)$ has a diagonal structure.

Once the system is converted to be a just proper one, additional frequency weighting $F_{W_i}(s)$ might be considered also, to shape the frequency behavior. The overall system is illustrated in Figure 2.

Denote the transfer function from u to $\tilde{y}$ by $T_{\tilde{y}u}$. Then it is shown that the following inequality holds:

$$||\Sigma(s)||_{-}^{[0,\bar{\omega}]} \geq \frac{||T_{\tilde{y}u}(j\omega)||_{-}^{[0,\infty]}}{\sup_{\omega\in[0,\bar{\omega}]} \bar{\sigma}[F_{W_i}(j\omega)F_M(j\omega)]}, \qquad (14)$$

where $||T_{\tilde{y}u}(j\omega)||_{-}^{[0,\infty]}$ can be calculated by (10). In other words, the above inequality provides a lower bound on the $\mathcal{H}_-$ norm of the strictly proper system, based on the augmented system and the filters. For further details see [8].

The values of κ and $F_{W_i}(s)$ can be selected based on the underlying application. For example if a certain frequency range $[0,\bar{\omega}]$ is of interest, than $F_{W_i}(s)$ can be chosen as a high-pass filter with gains big enough at frequencies above $\bar{\omega}$ and small enough at frequencies below $\bar{\omega}$.

The next section discusses the main contribution of the paper: the application of input and output blending for mode decoupling using the concepts introduced.

IV. Input and output blend calculation

A systematic input and output blend calculation is presented in the sequel. First the input blend, and then, in the second step the corresponding output blend is found.

A. Input blend

The aim of this subsection is to find an input blend vector k_u, which maximizes the excitation of a selected mode, while minimizes the impact on another one. The concept is shown in Figure 3. Here $\bar{u}$ is the scalar input from the $\mathcal{C}_i(s)$ SISO controller (see Figure 1), k_u is an m dimensional column vector distributing the blended input to the real input channels. Using our terminology the decoupling is formulated as: the sensitivity ($\mathcal{H}_-$ index) from $\overline{u}$ to the y_{p_i} performance output is to be maximized, while from $\overline{u}$ to y_{p_j} the worst case gain ($\mathcal{H}_\infty$ norm) should be minimized.

In order to account directly for the mode excitation, the sum of the states is connected to the output in the design phase. Therefore, the i^{th} complex mode is given by

$$\begin{aligned} \dot{x}_i(t) &= A_i x_i(t) + B_i u(t), \\ y_i(t) &= [\ 1 \quad 1\ ]\, x_i(t). \end{aligned} \qquad (15)$$

Since the modal states are related to the outputs without a direct feedthrough term the system is strictly proper and consequently the i^{th} mode has to be transformed into a just proper form by using the techniques described in section III-B.2. In addition $F_{W_j}(s)$ low pass filter can be introduced for shaping the frequency behavior of the j^{th} mode, as illustrated in Figure 3. Consequently, we introduce the shorthand notations of the augmented system's matrices as: $\hat{A}_{i,j}$, $\hat{B}_{i,j}$, $\hat{C}_{i,j}$, $\hat{D}_{i,j}$, which matrices include the dynamics of the filters and successively have non-zero direct feedthrough term.

Before putting everything together, we recall the fact that the norm of an LTI system Σ and its dual $\tilde{\Sigma}$ are the same. The dual system's matrices are defined by:

$$\tilde{A} = A^T, \quad \tilde{B} = C^T, \quad \tilde{C} = B^T, \quad \tilde{D} = D^T. \qquad (16)$$

Consequently, we use the dual representation for computing the input blend, for the following reasons. If one writes the LMIs (9) and (10) for the dual systems, and then substitutes back the augmented system's matrices based on (16), than this yields

$$\begin{bmatrix} P\hat{A}_i^T + \hat{A}_i P + \hat{B}_i K_u \hat{B}_i^T & P\hat{C}_i^T + \hat{B}_i K_u \hat{D}_i^T \\ \hat{C}_i P + \hat{D}_i K_u \hat{B}_i^T & \hat{D}_i K_u \hat{D}_i^T - \beta^2 I \end{bmatrix} \succ 0, \qquad (17)$$

and

$$\begin{bmatrix} Q\hat{A}_j^T + \hat{A}_j Q + \hat{B}_j K_u \hat{B}_j^T & Q\hat{C}_j^T + \hat{B}_j K_u \hat{D}_j^T \\ \hat{C}_j Q + \hat{D}_j K_u \hat{B}_j^T & \hat{D}_j K_u \hat{D}_j^T - \gamma^2 I \end{bmatrix} \preceq 0. \qquad (18)$$

Here we have introduced a new matrix variable $K_u = k_u \cdot k_u^T$, as the dyadic product of the input blend vector.

It is clear that these terms appearing in the LMIs only because of the dual representation, otherwise we would be facing a bilinear (and quadratic) matrix problem, i.e. the dual form ensures linearity. Nevertheless, the newly introduced variable K_u is a rank 1 matrix, which has to be taken into consideration. This is done by the simple and effective heuristic proposed by [12]: the minimization of the rank of a symmetric positive definite matrix, is the minimization of its nuclear norm, expressed by its trace.

Therefore, in order to find the optimal k_u input blend, one has to simultaneously maximize β subject to (17) and minimize γ subject to (18). The optimization variables are P, Q, K_u, β and γ, with K_u being a symmetric, rank 1 matrix. The optimization problem to be solved is

$$\begin{aligned} &\text{minimize} \quad -\beta^2 + \text{trace}(K_u) + \gamma^2 \\ &\text{subject to (17), (18)} \quad \text{and } 0 \preceq K_u \preceq I,\ Q \succeq 0, \end{aligned} \qquad (19)$$

with I being the identity matrix with appropriate dimensions.

Once (19) is solved, the input blend can be found by the Singular Value Decomposition (SVD) of K_u, which has only one non-zero singular value. The k_u blend vector is then given as the left singular vector corresponding to the non-zero singular value. Note that the additional constraint of $0 \preceq K_u \preceq I$ ensures normalized blending vectors.

Once k_u is found, it is applied to the given modes, e.g. for the i^{th} mode to give $\bar{A}_i = A_i$, $\bar{B}_i = B_i k_u$, $\bar{C}_i = C_i$, $\bar{D} = D k_u$. This formulation is then used for determining the corresponding output blend, as discussed next.

B. Output blend

Next, our aim is to find a linear combination of the available outputs such that the desired mode is observed as much as possible, while the other mode appears as less

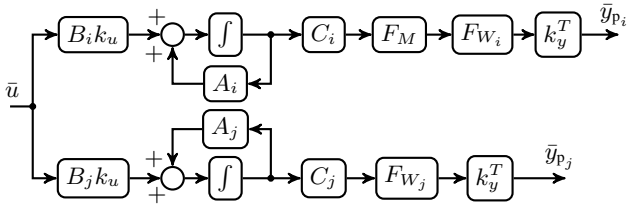

Fig. 4. Output blend calculation

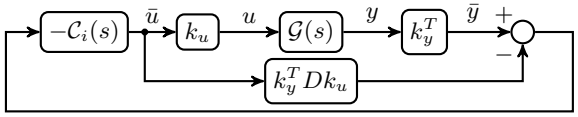

Fig. 5. Modified closed loop control of a given mode

as possible. Using the introduced terms, k_y^T should create a single blended output for the i^{th} mode with maximal sensitivity on its performance output, and minimal transfer on the j^{th} one. The approach is similar to the input blend calculation. The process is summarized in Figure 4.

The LMI constraints in the optimization for the i^{th} and j^{th} modes are readily given as

$$\begin{bmatrix} \hat{A}_i^T P + P\hat{A}_i + \hat{C}_i^T K_y \hat{C}_i & P\hat{B}_i + \hat{C}_i^T K_y \hat{D}_i \\ \hat{B}_i^T P + \hat{D}_i^T K_y \hat{C}_i & \hat{D}_i^T K_y \hat{D}_i - \beta^2 \end{bmatrix} \succ 0 \quad (20)$$

and

$$\begin{bmatrix} \hat{A}_j^T Q + Q\hat{A}_j + \hat{C}_j^T K_y \hat{C}_j & Q\hat{B}_j + \hat{C}^T K_y \hat{D}_j \\ \hat{B}_j^T Q + \hat{D}_j^T K_y \hat{C}_j & \hat{D}_j^T K_y \hat{D}_j - \gamma^2 \end{bmatrix} \preceq 0. \quad (21)$$

Here we introduced the output blend matrix $K_y = k_y \cdot k_y^T$. The $\hat{\cdot}$ notation symbols that frequency weights has been applied again as shown in Figure 4. Multiplicative frequency correction is necessary to the i^{th} mode, despite that the mode is already proper, with $\bar{D} = Dk_u$. In fact the direct feedthrough term needs to be zeroed out for both the i^{th} and j^{th} modes, and then frequency weighted augmentation with appropriate $F_M(s)$, $F_{W_i}(s)$ and $F_{W_j}(s)$ transfer functions are suggested (see Figure 4). The necessity of this correction lies in the fact that the direct feedthrough term is the same for all dynamical modes. Therefore, using the Schur lemma [10], the lower right blocks of (20) and (21) with the blended direct feedthrough matrices imply the followings:

$$\bar{D}^T K_y \bar{D} - \beta^2 \succ 0, \quad \bar{D}^T K_y \bar{D} - \gamma^2 \preceq 0 \quad (22)$$

It is easy to notice that $D^T K_y D$ serves as an upper bound for β^2 which should be maximized, and it is also a lower bound for γ^2 which should be minimized. This leads to contradiction, which can be overcome by removing the $\bar{D}$ term and apply suitable frequency weights as shown in Figure 4. Once the k_y input blend is found than $k_y^T D_i k_u = k_y^T D_j k_u$ and this effect can be removed from the measurements by a feed forward compensation term. In this case the control structure for the i^{th} mode is shown in Figure 5.

The optimization problem for finding the optimal k_y output blend, with variables P, Q, K_y, β, γ is given as follows. Find $P = P^T$, $Q = Q^T$, $K_y = K_y^T$ to

$$\begin{aligned} &\text{minimize} \quad -\beta^2 + trace(K_y) + \gamma^2 \\ &\text{subject to (20), (21) and } 0 \preceq K_y \preceq I,\ Q \succeq 0. \end{aligned} \quad (23)$$

The k_y vector can be retrieved from the SVD of K_y similarly as k_u in section IV-A.

Once the output blend is found, it is applied to the given modes, e.g. for the i^{th} mode to give

$$\begin{aligned} \dot{x}_i(t) &= A_i x_i(t) + B_i k_u \bar{u}(t), \\ \bar{y}_i(t) &= k_y^T C_i x_i(t) + k_y^T D k_u \bar{u}(t). \end{aligned} \quad (24)$$

V. Numerical examples

This section presents two numerical examples from the aerospace engineering field in order to validate the proposed approach. The models are taken from the Flexop [13] project which aims to design and demonstrate flutter suppression techniques on a demonstrator UAV.

The dynamical model has two flutter modes arising from the coupling of aerodynamic and structural forces. These modes become unstable over a certain airspeed. We have selected the stable LTI representation at speed $47\frac{m}{s}$ to illustrate our blending approach (for more details about the modeling we refer to [14]). A lower order representation is obtained first, which is then transformed into the modal form.

The demonstrator aircraft is equipped with eight ailerons (four on the left and four on the right wings) and two ruddervators on each side. Measurements are given at the 90% spanwise location on the left and right trailing edge, providing information about the vertical acceleration (a_z) and the angular rates (ω_x, ω_y) around the lateral and longitudinal axis of the aircraft respectively.

The first example involves only rigid body modes, and it aims to present an easy to evaluate example for the input and output blend calculation. The sensitivity of the roll subsidence mode is increased, while having a minimal impact on the short period mode. The roll subsidence is a lateral mode which involves roll rate and roll angle, and controlled by lateral control inputs (mainly ailerons). The short period mode is a well damped oscillatory mode corresponding to the longitudinal dynamics of the aircraft, strongly affected by elevator deflections. Because the two modes are lightly coupled, it is expected that the lateral control inputs will dominate the input blend vector.

The input and output blends were calculated according to (19) and (23) respectively. The $F_M(s)$ filter was selected to have a zero at the natural frequency of the mode to be controlled, i.e. in (13) κ is selected as the natural frequency of the selected mode, with value $\omega_n = 22.6\frac{rad}{s}$. The selection of κ defines the frequency band, where the mode decoupling is guaranteed. According to [8] the $F_{W_i}(s)$ filter was selected as a high pass filter over the ω_n frequency. The $F_{W_j}(s)$ filter was selected as a low pass filter with cutoff frequency higher than the two mode's natural frequencies to exclude high frequency dynamics. The effect of the $F_{W_j}(s)$ filter's frequency band has been tested numerically by setting different frequency band values, but only minor changes in the k_u, k_y blend vectors were observable. The optimization problems were formalized using YALMIP, and the employed solver was SeDuMi.

	aileron		elevator	rudder
	left wing	right wing		
δ_1	-0.29	0.26	0.00	-0.06
δ_2	-0.41	0.39	-0.02	-0.10
δ_3	-0.38	0.41		
δ_4	-0.32	0.32		

TABLE I

CALCULATED INPUT BLEND FOR THE FIRST EXAMPLE

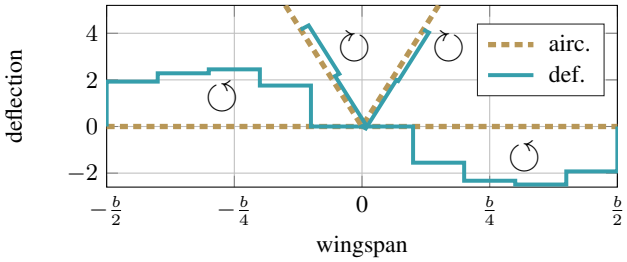

Fig. 6. Control surface deflection directions and relative magnitudes (b is the wing span)

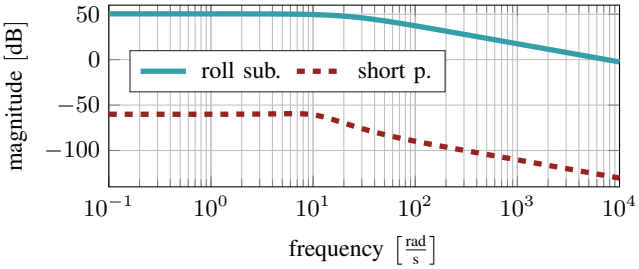

Fig. 7. Bode magnitude plot of the blended modes

	left wing	right wing
a_z	-0.69	0.72
ω_x	-0.01	-0.01
ω_y	-0.01	0.01

TABLE II

OUTPUT BLEND FOR THE FIRST EXAMPLE

Table I summarizes the input blend vector elements. [1] On the wings δ_i denotes the aileron deflections, with increasing indices from the wing root to the tip. In case of the ruddervators δ_1 denotes the lower one converted into elevator and rudder deflections, while δ_2 denotes the upper one. By comparing them, it is obvious that the results are according to our expectations. The blending gains for the lateral control inputs are relatively high compared to the elevator gains which are almost negligible.

A schematic sketch is given in Figure 6 about the control surface deflections (i.e. the elements of the input blend vector) and their induced rotation about the longitudinal axis of the aircraft. The aircraft nose points inward the paper. For representation purposes all deflections are multiplied by a constant scalar. The aileron defections are further multiplied by minus one, for depicting the real movement direction on the wing. The figure shows that aileron deflections are corresponding to a negative rolling moment, while the rudders are damping it with a light opposite directional effect. The two modes are originally lightly coupled, and the resulting input blend excites the lateral mode with lateral inputs, while providing reasonably small inputs to the longitudinal dynamics. It satisfies the previous expectations.

After the input blend step the $\mathcal{H}_-$ index was 2.15 and the $\mathcal{H}_\infty$ norm was 0.01. By applying an output blend the $\mathcal{H}_-$ index was further increased to 69.77, while the $\mathcal{H}_\infty$ norm did not change significantly. Figure 7 depicts the Bode magnitude plots for the input and output blended modes, when the direct feedthrough is removed. From these results it is obvious that a quasi perfect decoupling has been achieved on this simple example.

The second example considers two stable flutter (symmetric and antisymmetric) modes of the aircraft. Our aim is to control the antisymmetric mode, while leaving the symmetric one unaffected. We have compared the results by the one proposed by [7]. The latter method will be denoted by $\mathcal{H}_2$, as it applies an $\mathcal{H}_2$ norm based blend calculation, while the present approach will be denoted by $\mathcal{H}_{-/\infty}$.

The corresponding aileron input blends are collected in Table III. It can be observed that both methods select same directional deflections on each wing, except the ailerons at the tips, where they are deflected in opposite directions. In both approaches the rudder terms are more dominant, providing additional lateral inputs to the ailerons in order to successfully decouple the two modes. The rudder inputs are generating a sideslip motion, which results in antisymmetric lift distribution between the wings, and so further increase the control effectiveness on the antisymmetric mode. Table IV compares the output blend vectors.

The control surface deflections for both approaches are shown in Figure 8, which strengthens the similarity between the results. Difference can be observed at the outmost actuators, where the $\mathcal{H}_2$ method provides less deflection, while at the third actuator positions it gives larger deflections. Since the outmost actuators are damping the rolling effects created by the inner ones, the second approach results in a larger negative rolling moment.

Figure 9 compares the two approaches based on time domain simulation results, where doublet inputs were used for exciting the blended subsystems. It can be clearly seen that there is a significant difference in the open loop response

TABLE III

CALCULATED INPUT BLEND FOR THE SECOND EXAMPLE

	aileron				elevator		rudder	
	left wing		right wing					
	$\mathcal{H}_{-/\infty}$	$\mathcal{H}_2$	$\mathcal{H}_{-/\infty}$	$\mathcal{H}_2$	$\mathcal{H}_{-/\infty}$	$\mathcal{H}_2$	$\mathcal{H}_{-/\infty}$	$\mathcal{H}_2$
δ_1	-0.37	-0.38	0.38	0.38	0.002	0.001	-0.09	-0.09
δ_2	-0.44	-0.46	0.47	0.49	-0.01	-0.01	-0.17	-0.17
δ_3	-0.16	-0.22	0.23	0.28				
δ_4	0.35	0.26	-0.29	-0.21				

[1] In order to gain sufficient insight to the ruddervator blend, it is necessary to convert them to classical elevator and rudder inputs, where they can be separated to lateral (rudder) and longitudinal (elevator) inputs. The conversion is carried out based on [15].

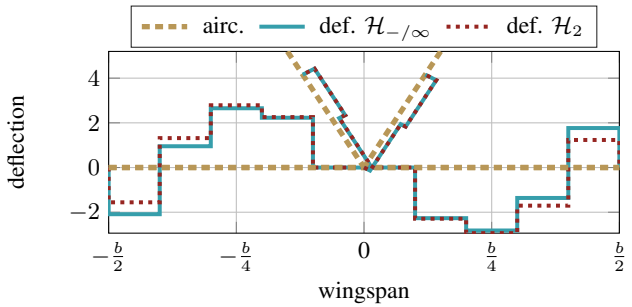

Fig. 8. Control surface deflection directions and relative magnitudes (b is the wing span)

	left wing		right wing	
	$\mathcal{H}_{-/\infty}$	$\mathcal{H}_2$	$\mathcal{H}_{-/\infty}$	$\mathcal{H}_2$
a_z	-0.54	0.67	0.78	0.63
ω_x	-0.04	0.04	-0.04	0.04
ω_y	0.22	-0.27	-0.24	0.27

TABLE IV
OUTPUT BLEND FOR THE SECOND EXAMPLE

of the two modes. The two approaches provided almost similar responses, with a slight difference in the symmetric flutter mode.

VI. CONCLUSIONS

An approach for individual control of selected mode(s) has been presented in the paper. It is based on the computation of the $\mathcal{H}_-$ index and $\mathcal{H}_\infty$ norm. They can be easily calculated through convex optimization subject to LMI constraints. When the given mode is strictly proper the introduction of a certain frequency correction method is necessary in order to calculate the $\mathcal{H}_-$ index over a finite frequency range. The presented technique is suitable for stable modes of LTI systems. In the introduced examples two rigid body and later two flutter modes were successfully decoupled. In the frame of the second numerical example it was shown that the presented method and the approach described in [7] yield similar results in terms of blend vectors and time domain simulation. The achievable level of decoupling for highly coupled systems should be analyzed in more details later.

However, the presented approach relies on Linear Matrix Inequality techniques, giving the opportunity for various extensions. It is our intention to include the use of Gramian based measures in our framework and compare it with the proposed $\mathcal{H}_\infty$ metric. Then, the question of unstable systems will be investigated through co-prime factorization and generalized Gramians. The method has also the advantage of straightforward extension for the case of multiple modes by simply increasing the corresponding LMI constraints in the optimization. Last but not least, the mathematical tools employed in the paper are scalable for Linear Parameter Varying plants, with some technical details to be worked out in the near future.

ACKNOWLEDGEMENT

The research leading to these results is part of the FLEXOP project. This project has received funding from the European Unions Horizon 2020 research and innovation programme under grant agreement No 636307. This paper was supported by the János Bolyai Research Scholarship of the Hungarian Academy of Sciences. The research reported in this paper was supported by the Higher Education Excellence Program of the Ministry of Human Capacities in the frame of Artificial Intelligence research area of Budapest University of Technology and Economics (BME FIKPMI/FM).

The research was supported by the NKP-18-3 and the NKP-18-4 New National Excellence Programs of the Ministry of Human Capacities.

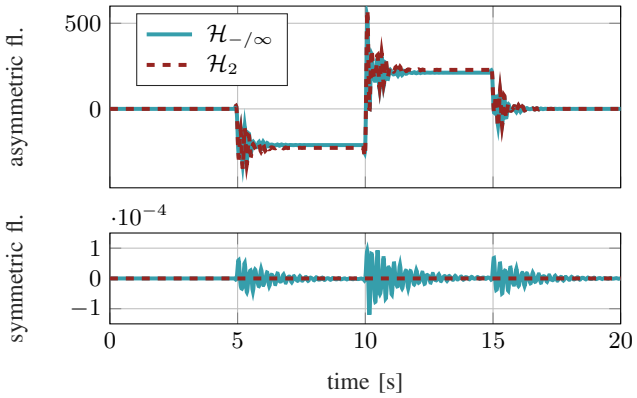

Fig. 9. Output excitation

REFERENCES

[1] E. G. Gilbert, "The decoupling of multivariable systems by state feedback," *SIAM Journal on Control*, vol. 7, no. 1, pp. 50–63, 1969.
[2] W. Gawronski, *Advanced structural dynamics and active control of structures*. Springer Science & Business Media, 2004.
[3] A. Schirrer, C. Westermayer, M. Hemedi, and M. Kozek, "Actuator and sensor positioning optimization in control design for a large BWB passenger aircraft," *ISRN Mechanical Engineering*, vol. 2011, 2011.
[4] T. Nestorović and M. Trajkov, "Optimal actuator and sensor placement based on balanced reduced models," *Mechanical Systems and Signal Processing*, vol. 36, no. 2, pp. 271–289, 2013.
[5] W. Gawronski and K. Lim, "Balanced actuator and sensor placement for flexible structures," *International Journal of Control*, vol. 65, no. 1, pp. 131–145, 1996.
[6] B. P. Danowsky, P. Thompson, D.-C. Lee, and M. J. Brenner, "Modal isolation and damping for adaptive aeroservoelastic suppression," in *AIAA Atmospheric Flight Mechanics (AFM) Conference*, 2013, p. 4743.
[7] M. Pusch, "Aeroelastic mode control using H2-optimal blends for inputs and outputs," in *2018 AIAA Guidance, Navigation, and Control Conference*, 2018, p. 0618.
[8] J. Liu, J. L. Wang, and G.-H. Yang, "An LMI approach to minimum sensitivity analysis with application to fault detection," *Automatica*, vol. 41, no. 11, pp. 1995–2004, 2005.
[9] S. Skogestad and I. Postlethwaite, *Multivariable feedback control: analysis and design*. Wiley New York, 2007, vol. 2.
[10] C. Scherer and S. Weiland, "Linear matrix inequalities in control," *Lecture Notes, Dutch Institute for Systems and Control, Delft, The Netherlands*, vol. 3, p. 2, 2000.
[11] J. L. Wang, G.-H. Yang, and J. Liu, "An LMI approach to H_- index and mixed H_-/H_∞ fault detection observer design," *Automatica*, vol. 43, no. 9, pp. 1656–1665, 2007.
[12] M. Fazel, H. Hindi, and S. P. Boyd, "A rank minimization heuristic with application to minimum order system approximation," in *American Control Conference, 2001. Proceedings of the 2001*, vol. 6. IEEE, 2001, pp. 4734–4739.
[13] F. Consortium *et al.* (2015) The FLEXOP project. [Online]. Available: URL: https://flexop. eu. Accessed: 25 September 2018
[14] T. Luspay, T. Péni, and B. Vanek, "Control oriented reduced order modeling of a flexible winged aircraft," in *2018 IEEE Aerospace Conference*. IEEE, 2018, pp. 1–9.
[15] R. W. Beard and T. W. McLain, *Small unmanned aircraft: Theory and practice*. Princeton University Press, 2012.